MAX-PLANCK-INSTITUT FÜR PHYSIK UND ASTROPHYSIK

WERNER-HEISENBERG-INSTITUT FÜR PHYSIK

MPI-PAE/Exp. El. 192
July 1988

PRODUCTION OF D, D^* AND D_s MESONS IN 200 GeV/c π^-, K^- AND p-Si INTERACTIONS

The ACCMOR Collaboration

Amsterdam[1)]-Bristol[2)]-CERN[3)]-Cracow[4)]-Munich[5)]-Rutherford[6)]-Valencia[7)] Collaboration

S. Barlag[5], H. Becker[5□], T. Böhringer[3Δ], M. Bosman[3↔], V. Castillo[3%], V. Chabaud[3], D. Buchholz[5§], C. Damerell[6], C. Daum[1], H. Dietl[5], H. Fawcett[2], S. Gill[6], A. Gillman[6], R. Gilmore[2], T. Gooch[2], L. Görlich[4], P. Gras[7], Z. Hajduk[4], E. Higon[7], B.D. Hyams[3], D.P. Kelsey[3#], J. Kemmer[8], R. Klanner[5∇], U. Kötz[3†], S. Kwan[2x], B. Lücking[5], G. Lütjens[5], G. Lutz[5], J. Malos[2], W. Männer[5], E. Neugebauer[5@], H. Palka[5*], M. Pepé[6], J. Richardson[6], G. De Rijk[1x], K. Rybicki[4], H.J. Seebrunner[5&], U. Stierlin[5], H.G. Tiecke[1], M. Turala[4], G. Waltermann[5], S. Watts[6], P. Weilhammer[3], F. Wickens[6], L.W. Wiggers[1], M. Witek[4], A. Wylie[5], and T. Zeludziewicz[4]

ABSTRACT

The NA32 experiment at the CERN SPS has collected 38 million hadronic interactions with incident 200 GeV/c π^-, K^- and p beam. Using a segmented silicon active target and a telescope of high resolution silicon microstrip counters we have selected fully reconstructed $D^o \to K^-\pi^+$, $D^o \to K^-\pi^+\pi^+\pi^-$, $D^+ \to K^-\pi^+\pi^+$, $D_s^+ \to K^-K^+\pi^+$ and charge conjugate decays. The integrated cross-sections for D^o, D^+ D^{*+} and D_s^+ meson production and the dependence of the cross-section on longitudinal and transverse momentum of the D are presented.

To be submitted to Zeitschrift für Physik C

1) NIKHEF-H, Amsterdam, The Netherlands
2) University of Bristol, Bristol, UK
3) CERN, Geneva, Switzerland
4) Institute of Nuclear Physics, Cracow, Poland
5) Max Planck Institut für Physik, Munich, Fed. Rep. Germany
6) Rutherford Appleton Laboratory, Chilton, Didcot, UK
7) IFIC, CSIC and University of Valencia, Valencia, Spain
8) Technische Universität, Munich, Fed. Rep. Germany
□) Visitor from Gesamthochschule, Saarbrücken, Fed. Rep. Germany
Δ) Now at University of Lausanne, Lausanne, Switzerland
↔) Now at MPI, Munich, Fed. Rep. Germany
%) Now at University of Valencia, Valencia, Spain
§) Visitor from Northwestern University, Evanston, IL, USA
#) Now at Rutherford Appleton Laboratory, Chilton, Didcot, UK
∇) Now at DESY, Hamburg, Fed. Rep. Germany
†) Visitor from DESY, Hamburg, Fed. Rep. Germany
x) Now at CERN, Geneva, Switzerland
@) Now at Universität - GH Siegen, Siegen, Fed. Rep. Germany
*) Visitor from Institute of Nuclear Physics, Cracow, Poland
&) Now at Fachhochschule Heilbronn, Fed. Rep. Germany

8000 MÜNCHEN 40 - FÖHRINGER RING 6

Max-Planck-Institut für Physik und Astrophysik, München.

PRODUCTION OF D, D^* AND D_s MESONS IN 200 GeV/c π^-, K^- AND p-Si INTERACTIONS

The ACCMOR Collaboration

Amsterdam[1]-Bristol[2]-CERN[3]-Cracow[4]-Munich[5]-Rutherford[6]-Valencia[7] Collaboration

S. Barlag[5], H. Becker[5□], T. Böhringer[3Δ], M. Bosman[3↔], V. Castillo[3%], V. Chabaud[3], D. Buchholz[5§], C. Damerell[6], C. Daum[1], H. Dietl[5], H. Fawcett[2], S. Gill[6], A. Gillman[6], R. Gilmore[2], T. Gooch[2], L. Görlich[4], P. Gras[7], Z. Hajduk[4], E. Higon[7], B.D. Hyams[3], D.P. Kelsey[3#], J. Kemmer[8], R. Klanner[5∇], U. Kötz[3†], S. Kwan[2×], B. Lücking[5], G. Lütjens[5], G. Lutz[5], J. Malos[2], W. Männer[5], E. Neugebauer[5@], H. Palka[5*], M. Pepé[6] J. Richardson[6], G. De Rijk[1×], K. Rybicki[4], H.J. Seebrunner[5&], U. Stierlin[5], H.G. Tiecke[1], M. Turala[4], G. Waltermann[5], S. Watts[6], P. Weilhammer[3], F. Wickens[6], L.W. Wiggers[1], M. Witek[4], A. Wylie[5], and T. Zeludziewicz[4]

ABSTRACT

The NA32 experiment at the CERN SPS has collected 38 million hadronic interactions with incident 200 GeV/c π^-, K^- and p beam. Using a segmented silicon active target and a telescope of high resolution silicon microstrip counters we have selected fully reconstructed $D^o \to K^-\pi^+$, $D^o \to K^-\pi^+\pi^+\pi^-$, $D^+ \to K^-\pi^+\pi^+$, $D_s^+ \to K^-K^+\pi^+$ and charge conjugate decays. The integrated cross-sections for D^o, D^+ D^{*+} and D_s^+ meson production and the dependence of the cross-section on longitudinal and transverse momentum of the D are presented.

To be submitted to Zeitschrift für Physik C

1) NIKHEF-H, Amsterdam, The Netherlands
2) University of Bristol, Bristol, UK
3) CERN, Geneva, Switzerland
4) Institute of Nuclear Physics, Cracow, Poland
5) Max Planck Institut für Physik, Munich, Fed. Rep. Germany
6) Rutherford Appleton Laboratory, Chilton, Didcot, UK
7) IFIC, CSIC and University of Valencia, Valencia, Spain
8) Technische Universität, Munich, Fed. Rep. Germany
□) Visitor from Gesamthochschule, Saarbrücken, Fed. Rep. Germany
Δ) Now at University of Lausanne, Lausanne, Switzerland
↔) Now at MPI, Munich, Fed. Rep. Germany
%) Now at University of Valencia, Valencia, Spain
§) Visitor from Northwestern University, Evanston, IL, USA
#) Now at Rutherford Appleton Laboratory, Chilton, Didcot, UK
∇) Now at DESY, Hamburg, Fed. Rep. Germany
†) Visitor from DESY, Hamburg, Fed. Rep. Germany
×) Now at CERN, Geneva, Switzerland
@) Now at Universität - GH Siegen, Siegen, Fed. Rep. Germany
*) Visitor from Institute of Nuclear Physics, Cracow, Poland
&) Now at Fachhochschule Heilbronn, Fed. Rep. Germany

1. INTRODUCTION

In the last ten years hadroproduction of charmed particles has been studied by many experiments at the CERN SPS and ISR, and at the FNAL Tevatron [1]. It has however been difficult to extract a clean charm signal from a huge combinatorial background since the total charm cross-section is more than a thousand times smaller than the inelastic cross-section at these energies.

Since 1980 the ACCMOR collaboration has pursued a program of hadroproduction of charm at the CERN SPS. In the first stage of the NA11 experiment 175 GeV/c π^-Be interactions were recorded with a single electron trigger. We have observed D meson signals upon a high background [2]. The combination of the single electron trigger with a silicon vertex detector in the second stage allowed us to obtain clean samples of D and D_s but with low statistics [3].

Here we report on new results derived from data collected by the NA32 experiment (successor to NA11) in 1984 with an interaction trigger and a finely segmented active silicon target. This paper is organized as follows. We first describe the experimental apparatus (section 2), the reconstruction and selection of events (section 3) and the acceptance calculations (section 4). Finally, we discuss the results on differential and total cross-sections of charm production with π^-, K^- and p beams (sections 5-7).

2. THE EXPERIMENT

The NA32 experiment was performed at the CERN SPS using the ACCMOR spectrometer in an unseparated hadron beam of 200 GeV/c. Two threshold Cerenkov counters (CEDARs) tagged the incoming beam particles. A schematic layout of the spectrometer is shown in Fig. 1. It consisted of two magnets (M1,M2) and 48 planes of drift chambers arranged in 4 groups (DC2,3A,3B,3C). Three multicellular Cerenkov counters (C1,C2,C3) were used to identify π,K,p in the momentum range 4-80 GeV/c. Details of the spectrometer can be found in Ref. 4.

2.1 The Target Area

An enlarged view of the target area is shown in Fig. 2. It consisted of a beam telescope, an active target and a vertex detector. The active target [4] is built out of 14 identical silicon microstrip detectors 280 μm thick separated by 220 μm. Each plane has 48 horizontal strips of 20 μm pitch; each strip is connected to a charge sensitive preamplifier. The resulting measurement accuracy is 3 μm for isolated tracks. The 14 detectors are followed at a distance of 35 mm by two large silicon microstrip detectors with 400 μm pitch (multiplicity counters).

Measurement of coordinates of forward going particles are performed by a telescope of 7 silicon microstrip detectors (20 µm strip pitch) with capacitive charge division readout [5]. Each third (sixth) strip in the inner (outer) region of the detectors is connected to an ADC. The resulting measurement accuracy is 4.3 µm (7.8 µm). The detectors are arranged in three pairs with strips at an angle of ±14° to the horizontal plane, and one detector has horizontal strips. The beam telescope in front of the active target consists of two planes of the same type as used in the vertex detectors and two planes of the same type as used in the active target.

With the full set-up the measurement precision for tracks reconstructed in each of the two ±14° detector projections at the position of the primary vertex was 13 µm plus a multiple scattering contribution of $\frac{90}{p(\mathrm{GeV/c})}$ µm, where p is the momentum of the particle.

2.2 The Data

Data were collected with an interaction trigger. The trigger required a beam particle to go through one of the 16 middle strips of the first active target counter. An interaction was defined as a pulse height corresponding to at least 3 minimum ionizing particles (m.i.p.) measured in one of the central 16 strips of the active target planes 2 to 7. A multiplicity of at least three charged particles had to be confirmed in the multiplicity counters. During 1984, a total of 38.5 million triggers were collected : 22 million with a π^- beam, 5.5 million with a K^- beam and 11 million with a p beam.

3. RECONSTRUCTION AND SELECTION OF EVENTS

3.1 Preselection

To reduce the computer time needed for data processing, we preselected events on the basis of information from the active target and vertex detector only [4]. The primary vertex is reconstructed. Events were selected which contained at least two track projections of ±14° displaced from the primary vertex : the cut applied on the impact parameter was about 40 µm. This has to be compared with the average impact parameter between 30 µm and 300 µm for particles originating from decays of particles with a lifetime of $\sim 10^{-13}$-10^{-12}s. In order to avoid losses at small distances, events exhibiting an effective jump in charged particle multiplicity of at least 2 m.i.p. in the active target have also been accepted. Secondary interactions in the active target identified by a pulse height of more than 10 m.i.p. in a strip were rejected. The preselection reduces the data by a factor of 4.5.

3.2 Track and Vertex Reconstruction

For the preselected events, the tracks are reconstructed in the drift chambers. The information from the Cerenkov counters is used to identify particles [4]. A secondary vertex search is then performed using drift chamber tracks to guide the pattern recognition in the vertex detector. This secondary vertex search is restricted to track combinations in the $K^-\pi^+$, $K^-\pi^+\pi^+$, $K^-\pi^+\pi^+\pi^-$, $K^+K^-\pi^+$ and $pK^-\pi^+$ channels with invariant mass within 250 MeV/c^2 *) from the D^o, D^+, D_s or Λ_c mass **) [6]. To obtain a clean sample of fully reconstructed D decays, we apply the following criteria to select secondary vertices :

a) a good fit (90% C.L.) to a secondary vertex separated from the primary vertex by more than 2 mm (3 mm for the charged D),

b) the sum of the momentum vectors of the decay tracks has to point to the primary vertex (90% C.L.),

c) all decay tracks have to miss the primary vertex: the distance to the primary vertex, in one of the ±14° projections, of the extrapolated track has to be more than 1σ (2σ for D^+), where σ is the error on the impact parameter. In addition one track (two for 3-, 4-body decays) has to miss the primary vertex by 3σ.

The confidence level associated with the first two criteria is reduced to 80% for the proton data and all the $D^o \to K\pi\pi\pi$ decays because of higher combinatorial background.

The invariant mass distribution for the selected events is presented in Fig. 3. For π^-, K^- and proton data clear D meson signals appear on a low background. A total of 157 D^o and D^+ decays are observed: 114 with π^-, 34 with K^- and only 9 with p beam. A D_s signal is seen only for the K^- beam. No clear $\Lambda_c \to pK\pi$ signal was observed.

4. ACCEPTANCE CALCULATIONS

In order to study the production characteristics of D mesons, we have to correct the data for the acceptance in x_F, the longitudinal momentum of the D in the centre of mass system divided by the maximum possible value, and in p_T the transverse momentum of the D relative to the incident beam.

---

*) a lower limit on the invariant mass is used in the $K^-\pi^+$ channel for the study of $D^{*+} \to D^o(K^-\pi^+\pi^o)+\pi^+$ decays (see section 7).

**) particles symbols stand for particles and antiparticles unless explicitly stated.

Acceptance curves were determined by a Monte Carlo program for the above-mentioned decay modes of charmed particles. The primary vertex is chosen randomly in one of the target planes with a transverse distribution corresponding to the beam shape. Since it is measured in the active target with a precision independent of the multiplicity of the event, only the track of the charmed particle is generated and the decay vertex is chosen on this track according to the lifetime distribution. Then the decay tracks are generated and traced through the vertex detector and the spectrometer. To reproduce the topological cuts applied during the data selection, only the error on the impact parameter has to be assigned to the track projections of the decay tracks. Using real tracks we have calculated the set of distributions of impact parameter error according to the number of coordinates in a view in the vertex telescope, the momentum of the track and the number of track segments in the drift chambers. The error on the impact parameter in the Monte Carlo program is then randomly generated according to the distribution of the relevant category. Multiple scattering is also taken into account.

The main features of the event selection in the Monte Carlo program are as follows :

1. The requirements on the separation of the primary and the secondary vertices, on the impact parameter, on the momentum and the number of coordinates of the decay tracks are the same as in the real event selection.
2. The requirements on the impact parameter applied in the final selection are more stringent than at the preselection level which hence introduces no loss. However, a residual effect is present due to the track reconstruction efficiency at the level of the preselection (93%). It is independent of the decay distance as we have checked using a sample of K_s^o decaying in front of the vertex detector and fulfilling our final selection criteria.
3. Efficiencies associated to χ^2 cuts (points a) and b) in section 3.2) contribute as global factors.
4. All decay tracks are traced through the magnets. They have to traverse at least the first group of drift chambers.
5. The K or p track must traverse the second magnet and the Cerenkov counters. The probability of the kaon or proton identification is calculated according to an experimentally determined efficiency curve. We used about 21,000 K^{*o} decays into $K^+\pi^-$ and about 8000 ϕ decays into K^+K^- to measure the efficiency of the kaon identification as a function of its momentum [4]. For the determination of the proton identification efficiency we used a sample of 3000 Λ^o decays.

Figure 4 shows the final acceptance for the considered decay modes as a function of x_F.

The impact parameter and momentum distributions of the decay tracks of charmed particles that fulfil the selection criteria in the Monte Carlo simulation agree well with the corresponding distributions of the real data sample.

5. DIFFERENTIAL CROSS-SECTION

The differential cross-section for D meson production is usually parametrized as follows :

$$d^2\sigma/dx_F dp_T^2 \sim (1-x_F)^n e^{-bp_T^2} \qquad (1)$$

The x_F and p_T^2 distributions for the three observed decay channels, corrected for their relative acceptance and branching ratio (see section 6), are shown in Figs. 5 and 6 for incident π^- and K^- beam. The background contribution, estimated from the events in side bands around the D mass peak, has been subtracted. The values of the parameters n and b are not determined by a χ^2 fit to that distribution but rather by a combined maximum likelihood fit to the invariant mass spectrum and the x_F or p_T^2 distribution uncorrected for acceptance. For the mass spectrum we assumed a Gaussian signal on a linear background. For the x_F and p_T^2 distribution we used respectively $A(x_F)(1-x_F)^n$ where $A(x_F)$ is the acceptance as a function of x_F and $Be^{-bp_T^2}$ where B is the acceptance factor that does not depend on p_T^2. A similar parametrization as for the signal (1) is used for the x_F and p_T^2 distribution of the background since it represents the background events quite well.

Table 1 summarizes the results of the fit. The K^- data show steeper distributions, both for x_F and p_T^2 than the π^- data. We used a single component fit to the x_F distribution for the π^- data. The data indicate however a systematic excess of events at low x_F. We fitted a two-component distribution with different slopes

$$d\sigma/dx_F = a_1(1-x_F)^{n_1} + a_2(1-x_F)^{n_2} \qquad (2)$$

Table 2 shows the results of that fit. The fit is represented by the dashed line in Fig. 5a. The confidence level associated to the χ^2 calculated for that parametrization improves slightly from 55% for a single component to 69%. The data suggests then a steep central component contributing about 35% of the total cross-section together with a rather flat component contributing 65%. However with the presently available statistics of 114 D events such a central component is not required. The EHS-LEBC collaboration has applied as well a two-component fit to their 360 GeV/c π^-p data on charm production [7]. The result of the fit to their 57 events is shown in Table 2. The confidence level associated to the χ^2 calculated for our data using their result is slightly worse but still acceptable (23% C.L.).

For the π^- data we have repeated the single component fit separately for leading (i.e. having a common quark with the beam particle) and non-leading D mesons. A leading sample contains D^0,D^- and $\bar{D}^0$ from D^{*-} decays, while $\bar{D}^0$, D^+ and D^0 from D^{*+} are non-leading. The fits (see Table 1 and Fig. 7a,b) show only a weak indication of a leading effect. The LEBC-EHS values are in good agreement with our experiment except for non-leading D's where they measure a steeper distribution with a value 2σ away from our fit [7]. For the K^- data only D^0 are leading candidates (4 events). There is no difference between leading and non-leading D's (see table 1).

In the $K^+K^-\pi^-$ channel, we observe a small but clear D_s signal for the K^- beam (Fig.3d). No signal is observed with the π^- beam. Since the K^- beam seems to favour D_s production we separated D_s^- and D_s^+ to study the influence of the incident s quark. There are 9 D_s^- and 5 D_s^+ candidates in the mass range 1.95-2.00 GeV/c^2 with an expected background contribution of 1 to 2 events. Figure 8 shows their x_F distribution corrected for acceptance. The D_s^- candidates show a harder x_F distribution than the D_s^+ (see table 1), an indication of a leading s quark effect for D_s production.

For the p induced interactions we obtain $n = 5.5\pm^{2.1}_{1.8}$ (see Fig. 9 and Table 1). This value agrees well with n = 4.9±0.5 obtained by the LEBC-EHS collaboration [8].

6. TOTAL CHARM CROSS-SECTION

To estimate the total inclusive D cross-section for $x_F > 0$, we use the result of the maximum likelihood fit for a single $(1-x_F)^n$ component. The statistical error comes from the error on the number of observed events and the uncertainty on the parameter n. The systematic error includes the uncertainty on the global efficiency factors (section 4), the D lifetimes and the attribution of the error on the impact parameter of the decay tracks in the Monte Carlo program. Varying the D lifetimes $\tau_{D^0} = 4.29\pm^{0.12}_{0.11}\cdot 10^{-13}$s, $\tau_{D^+} = 10.29\pm^{0.35}_{0.29}\cdot 10^{-13}$s from [9] within errors changes the acceptance by about 2%. The global efficiency factors contribute for 4%. The errors on the impact parameters of the decay tracks in the data and the Monte Carlo simulation agree within 10%. This corresponds to uncertainties in the acceptance of 2.5% for $K\pi$, 3.0% for $K\pi\pi$ and 8% for $K\pi\pi\pi$. The total systematic error amounts to 5-7%. A further check of our acceptance and the overall normalization was made by calculating the total inclusive K_s^0 cross-section based on 1800 K^0's decaying before the vertex telescope. Our value agrees well with the cross-section measured by other experiments [10-13]. The comparison is made in Table 3.

For the calculation of the cross-section we have used the recent MARK III branching ratios [14]: $BR(D^o \to K^-\pi^+) = (4.2\pm0.4\pm0.4)\%$, $BR(D^o \to K^-\pi^+\pi^+\pi^-) = (9.1\pm0.8\pm0.8)\%$ and $BR(D^+ \to K^-\pi^+\pi^+) = (9.1\pm1.3\pm0.4)\%$. The results are listed in Table 1 assuming a linear A depedence of the charm cross-section. An $A^{0.8}$ dependence (as discussed in ref. 1) would yield values larger by a factor of 2 than those in Table 1.

The value of :

$$\sigma(x_F>0)(\pi^-N\to D/\bar{D}+X) = (5.1\pm^{0.6}_{0.5}\pm0.3)\mu b/\text{nucleon}$$

should be compared with (25±4±11)μb/nucleon reported in a previous experiment (NA11) [3] for $D\bar{D}$ pair production for all x_F in π^--Be interactions. The uncertainty in the efficiency of the single electron trigger (0.11±0.04) and the assumption that only $D\bar{D}$ pairs are produced without correlation between the D's were the source of the relatively large systematic error. Using the latest branching ratios for the NA11 and the NA32 cross-sections the discrepancy is at the level of 2σ.

The D cross-section is slightly higher for the K^- beam than for the π^- beam when we compare the results for a single $(1-x_F)^n$ component :

$$\sigma(K^-N \to D/\bar{D}+X) \;/\; \sigma(\pi^-N \to D/\bar{D}+X) = 1.6\pm^{0.4}_{0.3} \quad ; \quad x_F > 0.$$

However, if we simply sum the cross-section bin by bin in the acceptance corrected x_F distribution (Fig. 5a, 5b), this ratio goes down to 1.2±0.4.

The D cross-section for proton beam is small (see Table 1). We find

$$\sigma(pN \to D/\bar{D}+X) \;/\; \sigma(\pi^-N \to D/\bar{D}+X) = 0.30\pm0.15.$$

Our value is in good agreement with the measurement of HOLEBC at the same energy [15] and the upper limit of our previous experiment [2]. Thus the proton induced D production is significantly reduced at 200 GeV/c, in contrast to the LEBC-EHS results from 360 GeV/c π^-p and 400 GeV/c pp data [7], giving similar cross-sections.

Large Λ_c cross-section in the forward region ($x_F > 0.5$) have been reported with proton beam at ISR energies [1] but also by the BIS-2 experiment at Serpukhov [16] with a neutron beam at a mean energy of 58 GeV/c. The sensitivity of our experiment to Λ_c is smaller than the sensitivity to D mesons essentially because of the much shorter Λ_c lifetime. The acceptance for the $\Lambda_c \to pK\pi$ decay mode is peaked towards high x_F values. We have searched for Λ_c in our proton data. To increase our sensitivity, we have, in addition to the kaons and protons identified by the Cerenkovs, considered all tracks with a momentum above 50 GeV/c as a kaon or proton candidate. The resulting acceptance is shown in Fig. 4. To reduce the background, we limited the search for Λ_c to the region $x_F > 0.5$. No signal is observed on top of a flat background of about 3 events per 10 MeV bin, our typical mass resolution. By scanning the events around the Λ_c mass we cannot exclude that 4 events could be good Λ_c candidates. This would correspond to $\sigma(x_F>0.5)\times BR(\Lambda_c \to pK\pi)$ = 2.8 or 3.6 µb/silicon nucleus for a flat x_F or a $(1-x_F)^3$ distribution respectively. The BIS-2 experiment measures $\sigma(x_F>0.5)\times BR(\Lambda_c \to \Lambda^o\pi\pi\pi)$ = 2.3±1.1 µb/carbon nucleus. Using their measured $A^{0.73}$ dependence, BIS-2 would predict $\sigma(x_F>0.5)\times BR(\Lambda_c \to \Lambda^o\pi\pi\pi)$ = 4.3±2.0 µb/silicon nucleus. The decay modes $\Lambda_c \to Kp\pi$ and $\Lambda_c \to \Lambda^o\pi\pi\pi$ have similar branching ratios [9], there is thus no contradiction between our result and their measurement, although one could expect an increase in cross-section while going from 58 to 200 GeV/c for the incident beam energy. However BIS-2 measures $\sigma_{\bar{D}^o}(x_F>0.5)$ = 28±14 µb/carbon nucleus and $\sigma_{D^-}(x_F>0.5)$ = 26±13 µb/carbon nucleus. Using an $A^{0.73}$ dependence they would predict $\sigma_{\bar{D}^o+D^-}(x_F>0.5)$ = 102±36 µb/silicon nucleus. We have observed 2 $D^- \to K\pi\pi$ decay candidates and 2 $\bar{D}^o \to K\pi\pi\pi$ decay candidates above $x_F > 0.5$, accepting also tracks with momentum larger than 50 GeV/c as kaon candidate. This corresponds only to a cross-section of $\sigma_{\bar{D}^o+D^-}(x_F>0.5)$ = 3.1 µb/silicon nucleus, more than an order of magnitude lower than the BIS-2 value.

In the invariant mass distribution for the $K^-K^+\pi^+$ mass combination a clear D_s peak appears in the K^- data while no equivalent structure is observed in the π^- data. The signal observed in the K^- data corresponds to $\sigma(x_F>0)(K^-N \to D_s^\pm+X)\times BR(D_s \to KK\pi) = 0.24\pm^{0.10}_{0.06}\pm0.02$ µb for n = 1.1, the value obtained when fitting D_s^- and D_s^+ together (Table 1).
The upper limit for D_s production in the π^- beam is found to be :

$$\sigma(x_F>0)(\pi^-N\to D_s^\pm+X)/\sigma(x_F>0)(K^-N\to D_s^\pm+X) < 0.1 \quad (90\%\text{C.L.})$$

provided the $d\sigma/dx_F$ distributions are described by the same value of n.

Table 4 shows some ratios of cross-sections separately for π^- and K^- data. The values for the π^- beam are consistent with those of NA11 [3] and LEBC-EHS [7].

7. THE $D^{*\pm}$(2010) PRODUCTION IN π^--Si AND K^--Si INTERACTIONS

The following three decay channels were selected for the search of $D^{*\pm}$:

$$D^{*+} \to D^o\pi^+$$

with

$$D^o \to K^-\pi^+ \qquad (1)$$

$$D^o \to K^-\pi^+\pi^+\pi^- \qquad (2)$$

$$D^o \to K^-\pi^+\pi^o \qquad (3)$$

The selection of D^{o} decays is done with the criteria described in section 3 except for the $D^{o} \rightarrow K^{-}\pi^{+}\pi^{o}$ channel where the requirement that the reconstructed $K^{-}\pi^{+}$ momentum should point to the primary vertex is relaxed to allow for one missing π^{o}. The D^{*+} is identified by measuring the mass difference Δm between $D^{o}\pi^{+}$ and D^{o}. For the decay mode (3) with missing π^{o} the Δm is calculated for visible particles only, and the invariant mass of $K^{-}\pi^{+}$ from the D^{o} decay is required to fall into the mass interval 1.45–1.70 GeV/c^{2}. The contribution from the $D^{o} \rightarrow K\pi\pi^{o}\pi^{o}$ decay mode is suppressed by the residual momentum sum cut and the visible mass cut. The background was estimated from the sample with the wrong charge for the additional pion coupled to D^{o}. The Δm distributions are shown in Fig. 10 and the numbers of events obtained for individual channels are listed in Table 5.

The x_F and p_T^2 distributions were fitted with the same parametrization as in section 5. The values are listed in Table 1. For π^- and K^- beam they are similar to the values obtained for D mesons. The acceptance corrected x_F distribution is shown in Fig. 11 for π^- beam. The full line indicates the fitted x_F dependence. Dividing the sample into leading and non-leading D^* for π^- data, we do not observe an indication of a leading effect. The results for π^- beam are in good agreement with NA11 [2,3] and LEBC-EHS [17].

Using the same assumptions as in the previous section, $BR(D^{*+} \rightarrow D^{o}\pi^{+})$ = 0.49±0.08 [6] and $BR(D^{o} \rightarrow K\pi\pi^{o})$ = (13.3±1.2±3)% [14] we have measured the total inclusive $D^{*\pm}$ cross-section for π^- and K^- beam. The values are listed in Table 1. The π^- cross-section is consistent with the value (2.3±1.0) μb/nucleon obtained at 200 and 250 GeV/c by Fitch et al. [18]. The cross-section for π^- and K^- beam are similar. The ratio of $(D^{*+} \rightarrow D^{o}+\pi^{+})$ to D^{o} (see Table 4) agrees with $0.24\pm^{0.09}_{0.06}$ reported at 360 GeV/c by the LEBC-EHS collaboration [17].

8. SUMMARY

A study of 38.5 million triggers collected in 1984 by the NA32 experiment using the high-precision silicon detectors led to the following results, using a linear A dependence and parametrizing the cross-sections by $(1-x_F)^n e^{-bp_T^2}$:

$$\sigma(x_F>0)(\pi^- N \rightarrow D/\bar{D}+X) = (5.1\pm^{0.6}_{0.5}\pm 0.3)\mu b/\text{nucleon}$$

$$\sigma(x_F>0)(K^- N \rightarrow D/\bar{D}+X) = (8.0\pm^{1.9}_{1.3}\pm 0.5)\mu b/\text{nucleon}$$

$$\sigma(x_F>0)(pN \rightarrow D/\bar{D}+X) = (1.5\pm 0.7\pm 0.1)\mu b/\text{nucleon}$$

$$\sigma(x_F>0)(\pi^- N \rightarrow D^{*\pm}+X) = (2.4\pm 0.6\pm 0.2)\mu b/\text{nucleon}$$

$$\sigma(x_F>0)(K^- N \rightarrow D^{*\pm}+X) = (3.4\pm 1.7\pm 0.3)\mu b/\text{nucleon}$$

$$\sigma(x_F>0)(K^- N \rightarrow D_s^{\pm}+X)\bullet BR(D_s \rightarrow KK\pi) = (0.24\pm^{0.10}_{0.06}\pm 0.02)\mu b/\text{nucleon}$$

The fit to the x_F distribution yields for D mesons: $n = 2.5\pm^{0.4}_{0.3}$ in π^--Si interactions, $n = 4.7\pm0.9$ in K^--Si interactions and $n = 5.5\pm^{2.1}_{1.8}$ in p-Si interactions. The results for $D^{*\pm}(2010)$ are $n = 2.8\pm^{1.1}_{0.9}$ for π^- and $n = 2.9\pm^{2.9}_{2.2}$ for K^-.

The fit to the p_T^2 distribution gives for D mesons $b = 1.06\pm^{0.12}_{0.11}$ for π^- interactions, $b = 2.7\pm^{0.7}_{0.5}$ for K^- interactions and $b = 1.4\pm^{0.6}_{0.4}$ for p interactions, while for $D^{*\pm}$ $b = 0.9\pm^{0.3}_{0.2}$ for π^- interactions and $b = 1.4\pm^{1.4}_{0.6}$ for K^- interactions. For D_s mesons in K^- interactions, the fit yields $n = 1.1\pm^{0.9}_{0.7}$ and $b = 0.6\pm0.2$.

We fitted separately x_F distributions for leading and non-leading particles. For π^- interactions we see a weak indication of a leading effect for D mesons only. For K^- interactions, we observe a much harder x_F distribution for the 9 D_s^- candidates than the 5 D_s^+ candidates which can be interpreted as an indication of a leading s quark effect.

We searched for Λ_c and $\bar{D}$ in our proton data. We give an upper limit of $\sigma_{\Lambda c}(x_F>0.5)\bullet BR(\Lambda_c\to pK\pi) = 3.6$ µb/silicon nucleus and $\sigma_{\bar{D}}(x_F>0.5) = 3.1$ µb/silicon nucleus. While our limit for Λ_c is not in contradiction with the BIS-2 result for a neutron beam of 58 GeV/c mean energy, the limit on $\bar{D}$ is more than an order of magnitude lower than their value.

Acknowledgements

We wish to thank Anita Bjorkebo and Helga Carstens for their indefatigable help in the data processing and Carole Ponting for her skillful typing of the manuscript.

REFERENCES

[1] For a recent review see S.P.K. Tavernier, Charmed and Bottom Flavoured Particle Production in Hadronic Interactions. Report on Progress in Physics 50 (1987) 1439.

[2] R. Bailey et al., Phys. Lett. 132B (1983) 230 & 237;
R. Bailey et al., Nucl. Phys. B239 (1984) 15.

[3] R. Bailey et al., Z. Phys. C30 (1986) 51;
H. Palka et al., Z. Phys. C35 (1987) 151;
H. Becker et al., Phys. Lett. 184B (1987) 277.

[4] S. Barlag et al., Z. Phys. C37 (1987) 17;
G. de Rijk, Ph.D. Thesis, University of Amsterdam, 1986.

[5] E. Belau et al., Nucl. Instrum. Methods 214 (1983) 253.

[6] Rev. of Particle Properties, Phys. Lett. 170B (1986).

[7] M. Aguilar-Benitez et al., Phys. Lett. 161B (1985) 400.

[8] M. Aguilar-Benitez et al., Phys. Lett. 189B (1987) 476.

[9] D. Hitlin, Weak Decays, invited talk at the 1987 Symposium on Lepton and Photon Interactions at High Energies, Hamburg, (27-31 July 1987), CALT-68-1472.

[10] N. Biswas et al., Nucl. Phys. B167 (1980) 41.

[11] D. Ljung et al., Phys. Rev. D15 (1977) 3163.

[12] D. Bogert et al., Phys. Rev. D16 (1977) 2098.

[13] K. Heller et al., Phys. Rev. D16 (1977) 2737.

[14] J. Adler et al., SLAC-PUB-4291, submitted to Phys. Rev. Lett.

[15] O. Erriquez et al., Phys. Scripta 33 (1986) 202.

[16] A.N. Aleev et al., JINR Preprint, June 30, 86;
A.N. Aleev et al., Z. Phys. C23 (1984) 333;
A.N. Aleev et al., Z. Phys. C37 (1988) 243.

[17] M. Aguilar-Benitez, Phys. Lett. 169B (1986) 106.

[18] [18] V.L. Fitch et al., Phys. Rev. D33 (1986) 486.

Table 1

Results of the fit for determining the production parameters n,b
and total cross-section σ

beam	D mesons	# of events	n	$b[GeV^{-2}]$	$\sigma(x_F>0)^{*)}$ [μb/nucleon]
π^-	all D	114	$2.5\pm^{0.4}_{0.3}$	$1.06\pm^{0.12}_{0.11}$	$5.1\pm^{0.6}_{0.5}\pm0.3$
	background		6.1 ± 0.6	$1.31\pm^{0.15}_{0.13}$	
	leading D	54	$2.1\pm^{0.5}_{0.4}$	$1.22\pm^{0.20}_{0.17}$	$2.3\pm^{0.4}_{0.3}\pm0.1$
	non-leading D	60	$3.3\pm^{0.6}_{0.5}$	$0.91\pm^{0.12}_{0.11}$	$3.2\pm^{0.5}_{0.4}\pm0.2$
	$\overset{(-)}{D}{}^{0}$	75			$3.3\pm^{0.5}_{0.4}\pm0.3$
	$D^{\pm}$	39			$1.7\pm^{0.4}_{0.3}\pm0.1$
	$D^{*\pm}$	46	$2.8\pm^{1.1}_{0.9}$	$0.9\pm^{0.3}_{0.2}$	$2.4\pm0.6\pm0.2$
	leading D^*	27	$4.7\pm^{1.9}_{1.6}$		
	non-leading D^*	19	$1.7\pm^{1.4}_{1.0}$		
K^-	all D	34	4.7 ± 0.9	$2.7\pm^{0.7}_{0.5}$	$8.0\pm^{1.9}_{1.3}\pm0.5$
	background		$4.9\pm^{0.9}_{0.8}$	1.5 ± 0.3	
	leading D	4	$4.6\pm^{3.5}_{2.4}$	$3.4\pm^{2.6}_{1.5}$	
	non-leading D	29	$4.7\pm^{0.9}_{0.8}$	$2.6\pm^{0.7}_{0.5}$	
	$\overset{(-)}{D}{}^{0}$	19			$3.9\pm^{1.5}_{0.9}\pm0.3$
	$D^{\pm}$	15			$4.1\pm^{1.2}_{0.9}\pm0.3$
	$D^{*\pm}$	8	$2.9\pm^{2.9}_{2.2}$	$1.4\pm^{1.4}_{0.6}$	$3.4\pm1.7\pm0.3$
	$D_s^{\pm}$	11	$1.1\pm^{0.9}_{0.7}$	0.6 ± 0.2	$(0.24\pm^{0.10}_{0.06}\pm0.02)^{**)}$
	D_s^{-}	7	$0.7\pm^{0.9}_{0.7}$	0.5 ± 0.2	
	D_s^{+}	4	$4.9\pm^{3.9}_{2.9}$	$1.0\pm^{0.9}_{0.6}$	
p	all D	9	$5.5\pm^{2.1}_{1.8}$	$1.4\pm^{0.6}_{0.4}$	$1.5\pm0.7\pm0.1$

*) the first error is statistical, the second systematic.

**) the value quoted for D_s is $\sigma(x_F>0)$ × Branching ratio ($D_s \to KK\pi$)

Table 2

Results of a two-component fit to the x_F distribution for the π^- data

Experiment	a_1	n_1	a_2	n_2
NA32 π^-Si 200 GeV/c	16.9±7.5	7.6±4.6	11.2±3.8	2.0±0.7
LEBC-EHS [6] π^-p 360 GeV/c	$107\pm^{39}_{37}$	$7.5\pm^{2.5}_{1.7}$	$5.4\pm^{6.0}_{3.8}$	$0.7\pm^{1.0}_{0.7}$

Table 3

Total inclusive K^o_s cross-section

Experiment	Reaction	Total inclusive K^o_s cross-section
NA32 with A^1 dependence*)	200 GeV/c π^-Si	2.9±0.3 mb/nucleon
NA32 with $A^{0.8}$ dependence		5.6±0.6 mb/nucleon
Ref. [10]	200 GeV/c π^-p	3.74±0.24 mb/nucleon
Ref. [11]	205 GeV/c π^-p	3.64±0.61 mb/nucleon
Ref. [12]	250 GeV/c π^-p	3.98±0.5 mb/nucleon

*) the A^α dependence has been measured to be α = 0.8±0.2 [13]. We give our value for α = 1 and α = 0.8.

Table 4

Ratios of total cross-sections

channels	π^- beam	K^- beam
leading $\overset{(-)}{D}$/non-leading $\overset{(-)}{D}$	0.7 ± 0.1	-
$\overset{(-)}{D}{}^o/D^\pm$	$1.9\pm^{0.5}_{0.4}$	$1.0\pm^{0.4}_{0.3}$
$(D^o+D^+)/(D^o+D^-)$	0.7 ± 0.1	$0.8\pm^{0.3}_{0.2}$
$(D^{*\pm}\rightarrow\overset{(-)}{D}{}^o+\pi^\pm)/\overset{(-)}{D}{}^o$	0.36 ± 0.10	$0.43\pm^{0.26}_{0.23}$

Table 5

Selection criteria for D^* and results for π^- beam

channel	m (charged) [MeV/c²]	Δm [MeV/c²]	No. of events signal	background
$K^-\pi^+ + K^-\pi^+\pi^+\pi^-$	1840–1890	143–148	24	3
$K^-\pi^+\pi^o$	1450–1700	< 152	40	15

Figure Captions

Fig. 1 Schematic layout of the NA32 spectrometer showing the target region (T), magnets (M), drift chambers (DC) and Cerenkov hodoscopes (C).

Fig. 2 View of the NA32 target region.

Fig. 3 Invariant mass distributions for accepted events for the three decay channels together ($K^-\pi^+$, $K^-\pi^+\pi^+$ and $K^-\pi^+\pi^-\pi^+$) for π^- beam (a), K^- beam (b) and p beam (c). Fig. 3d shows the invariant mass distribution for the selected events for the $K^+K^-\pi^+$ channel for K^- beam. The solid line is the result of a maximum likelihood fit (see text).

Fig. 4 Acceptance as a function of x_F for the two D^o decay modes (a) and for D^+, D_s and Λ_c decay modes (b).

Fig. 5 The differential x_F distributions of the D mesons for π^- beam (a) and K^- beam (b). The background contribution, estimated from side bands in the invariant mass distribution, has been subtracted. The solid line is the result of a maximum likelihood fit where $d\sigma/dx_F$ is parametrized by $(1-x_F)^n$. The dashed line in Figure 5a represents the result of a two-component fit of the form $d\sigma/dx_F = a_1(1-x_F)^{n_1} + a_2(1-x_F)^{n_2}$.

Fig. 6 The differential p_T^2 distribution of the D mesons for π^- beam (a) and K^- beam (b). The background contribution, estimated from side bands in the invariant mass spectrum, has been subtracted. The solid line is the result of a maximum likelihood fit where $d\sigma/dp_T^2$ is parametrized by $e^{-bp_T^2}$.

Fig. 7 The acceptance corrected x_F distributions of the leading D mesons (a) and non-leading D mesons (b). The background contribution, estimated from side bands in the invariant mass spectrum, has been subtracted. The solid line is the result of a maximum likelihood fit where $d\sigma/dx_F$ is parametrized by $(1-x_F)^n$.

Fig. 8 The acceptance corrected x_F distributions of the D_s^- mesons (a) and D_s^+ mesons (b) for the K^- data for $x_F > 0.1$.

Fig. 9 The differential x_F distributions of the D mesons for the proton data. The background contribution, estimated from side bands in the invariant mass spectrum, has been subtracted. The solid line is the result of a maximum likelihood fit where $d\sigma/dx_F$ is parametrized by $(1-x_F)^n$.

Fig. 10 a) Invariant mass distribution of the mass difference $\Delta m = m(K^-\pi^+\pi^+) - m(K^-\pi^+)$ or $\Delta m = m(K^-\pi^+\pi^-\pi^+\pi^+) - m(K^-\pi^+\pi^-\pi^+)$ for $m_{K^-\pi^+}$ or $m_{K^-\pi^+\pi^-\pi^+}$ in the D^o mass region for π^- and K^- data.

b) Invariant mass distribution of the mass difference $\Delta m = m(K^-\pi^+\pi^+) - m(K^-\pi^+)$ for $m_{K^-\pi^+}$ in the mass range 1.45–1.70 GeV/c^2 for π^- and K^- data. The dashed curve indicates the prediction from the Monte Carlo program

Fig. 11 The acceptance corrected x_F distributions for D^{*+} where $D^{*+} \to D^o \pi^+$ for the three D^o decay channels : (a) $D^o \to K^-\pi^+$, (b) $D^o \to K^-\pi^+\pi^-\pi^+$ and (c) $D^o \to K^-\pi^+\pi^o$ for π^- data. The background contribution, estimated from the wrong sign Δm distribution, has been subtracted. The solid line is the result of a fit where $d\sigma/dx_F$ is parametrized by $(1-x_F)^n$.

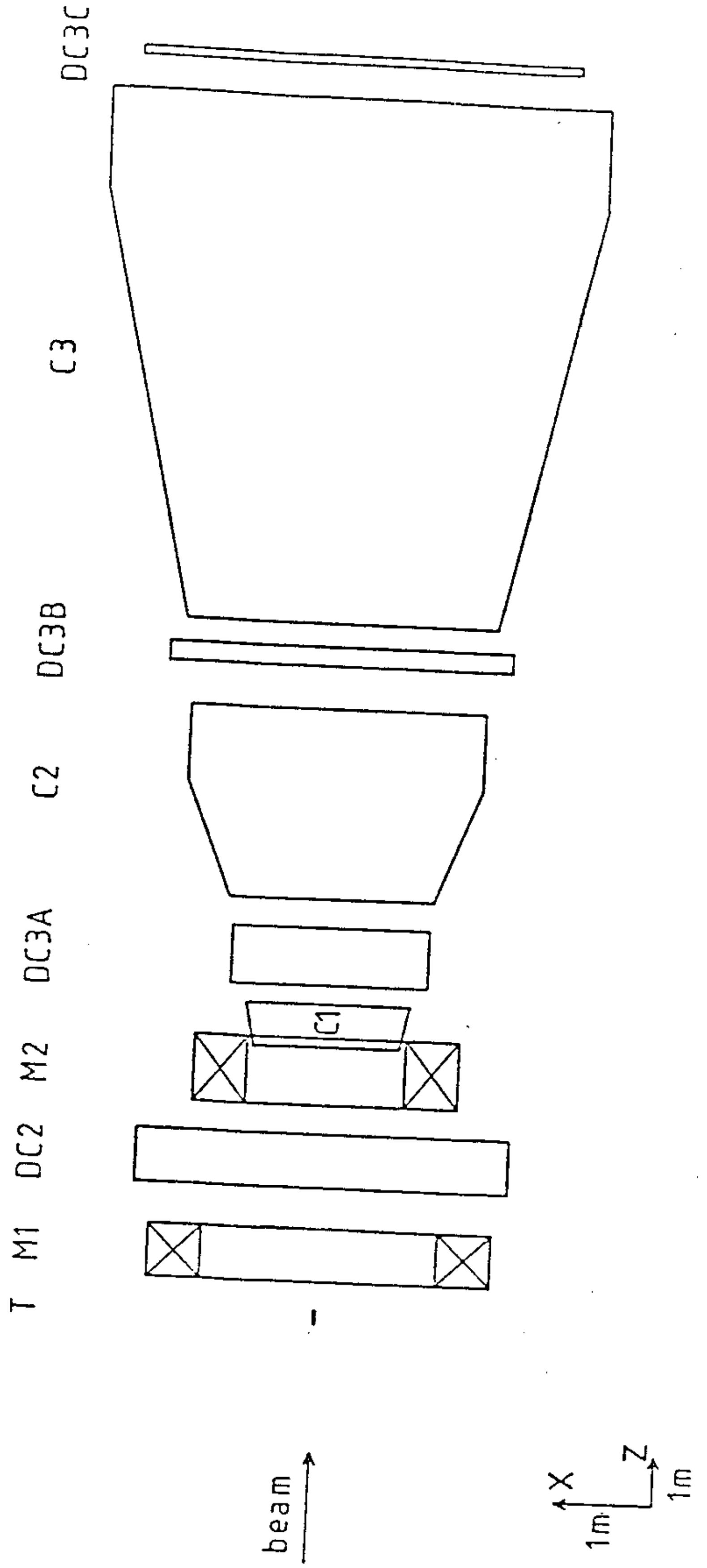

Fig.1

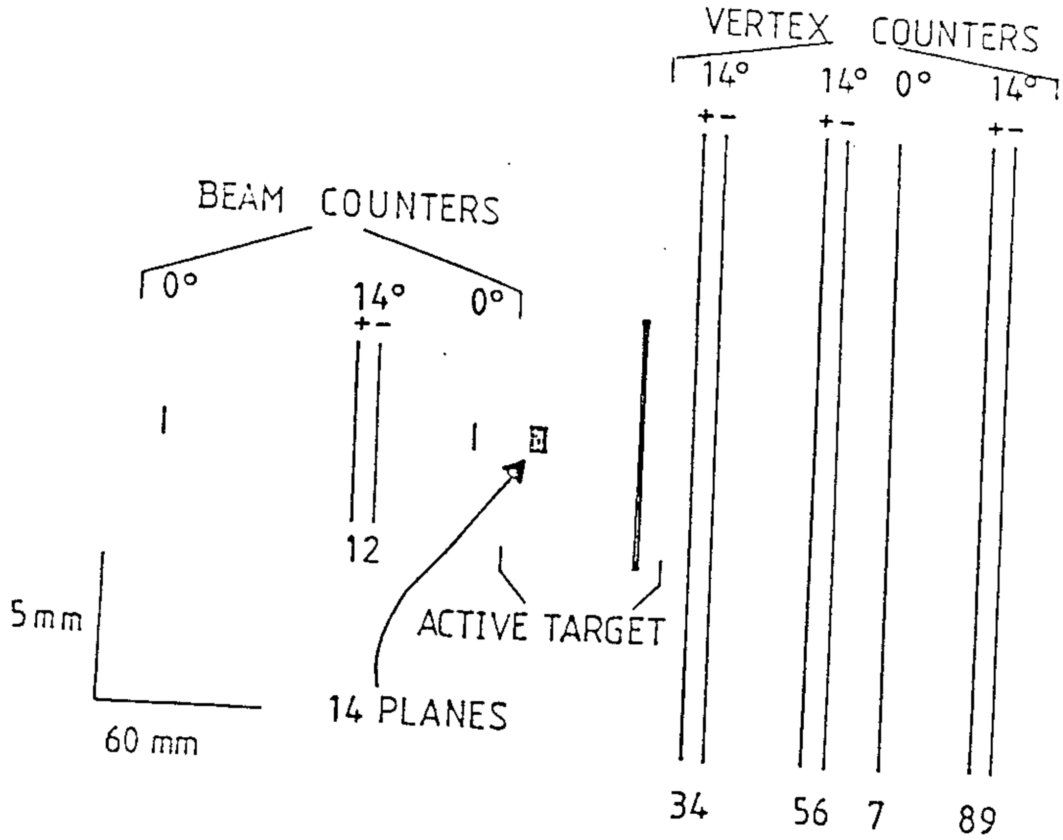
VERTEX COUNTERS
14°
14°
0°
14°
+ -
+ -
+ -
BEAM COUNTERS
0°
14°
0°
+ -
12
5mm
60 mm
ACTIVE TARGET
14 PLANES
34
56
7
89

Fig. 2

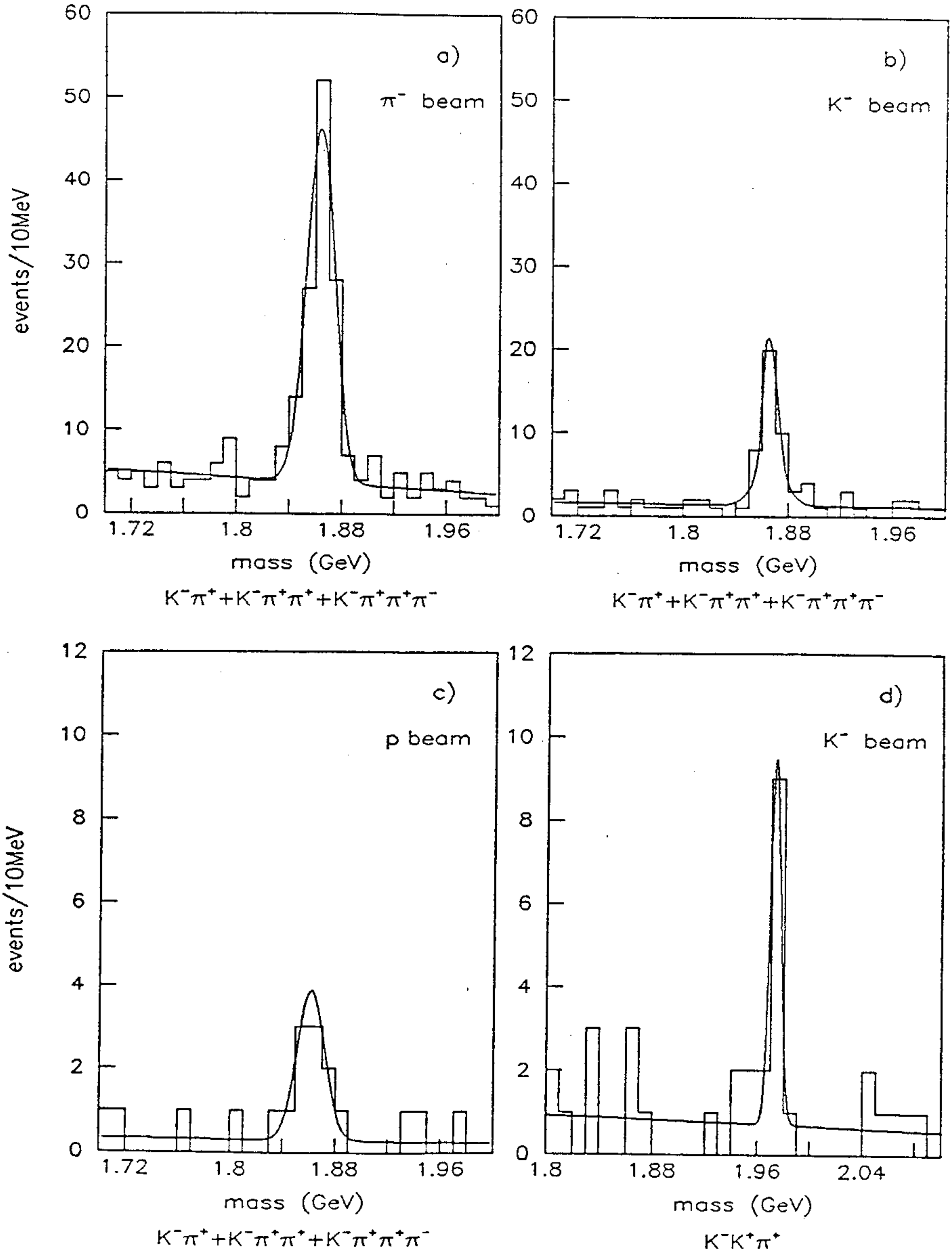
a)
π⁻ beam
events/10MeV
mass (GeV)
K⁻π⁺+K⁻π⁺π⁺+K⁻π⁺π⁺π⁻
b)
K⁻ beam
mass (GeV)
K⁻π⁺+K⁻π⁺π⁺+K⁻π⁺π⁺π⁻
c)
p beam
events/10MeV
mass (GeV)
K⁻π⁺+K⁻π⁺π⁺+K⁻π⁺π⁺π⁻
d)
K⁻ beam
mass (GeV)
K⁻K⁺π⁺

Fig.3

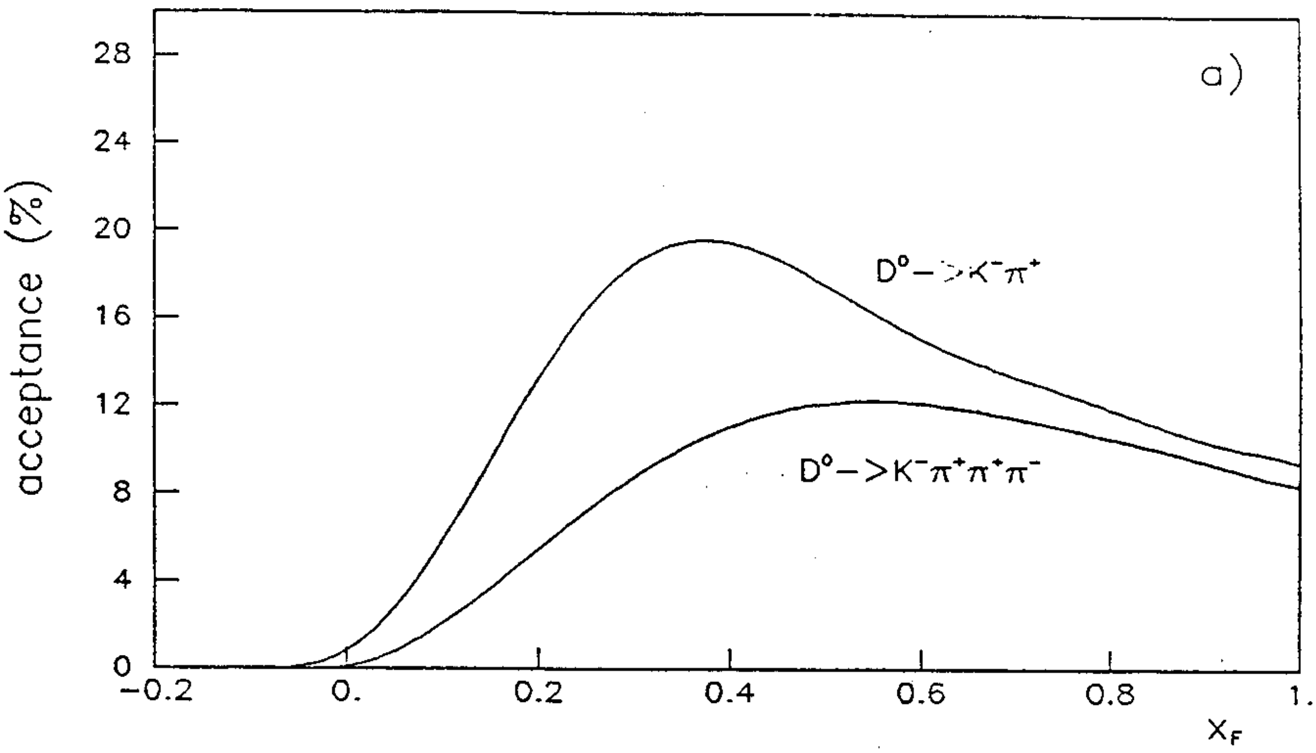
a)
acceptance (%)
28
24
20
16
12
8
4
0
−0.2
0.
0.2
0.4
0.6
0.8
1.
x_F
$D^0 \to K^-\pi^+$
$D^0 \to K^-\pi^+\pi^+\pi^-$

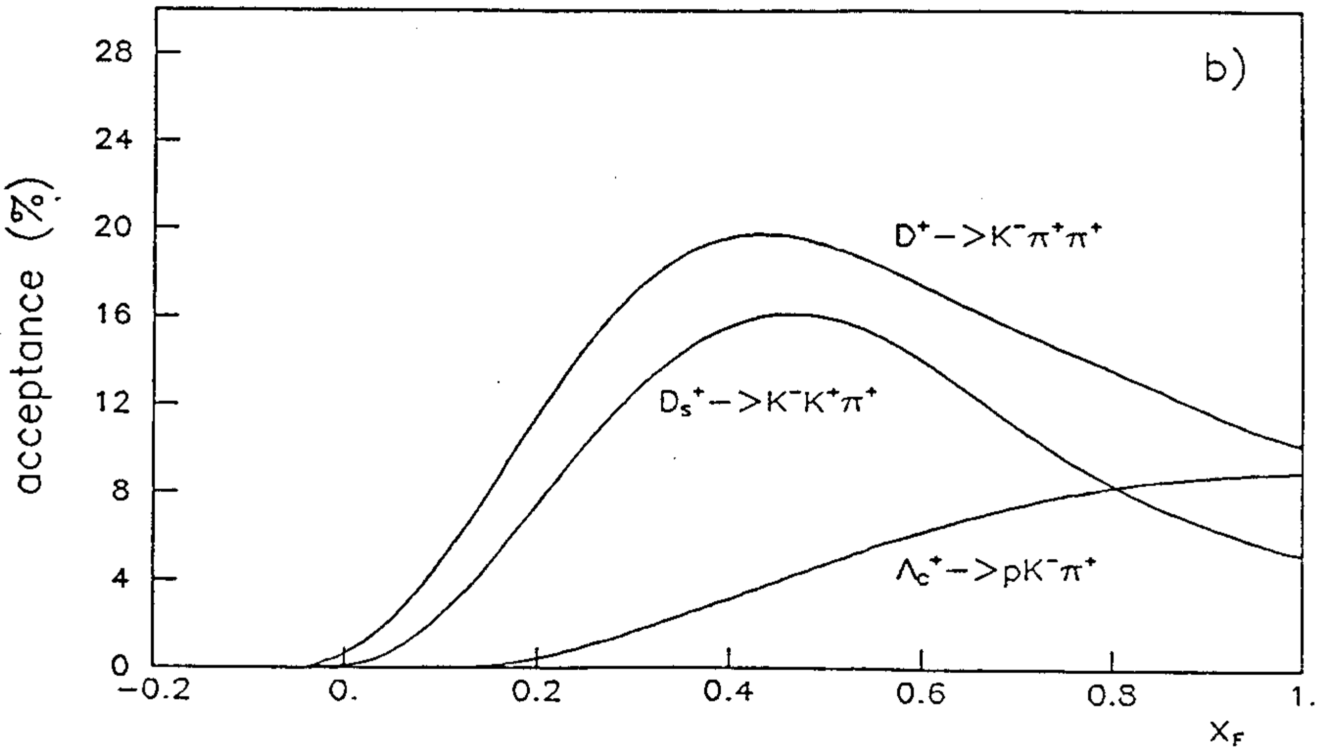
b)
acceptance (%)
28
24
20
16
12
8
4
0
−0.2
0.
0.2
0.4
0.6
0.8
1.
x_F
$D^+ \to K^-\pi^+\pi^+$
$D_s^+ \to K^-K^+\pi^+$
$\Lambda_c^+ \to pK^-\pi^+$

Fig.4

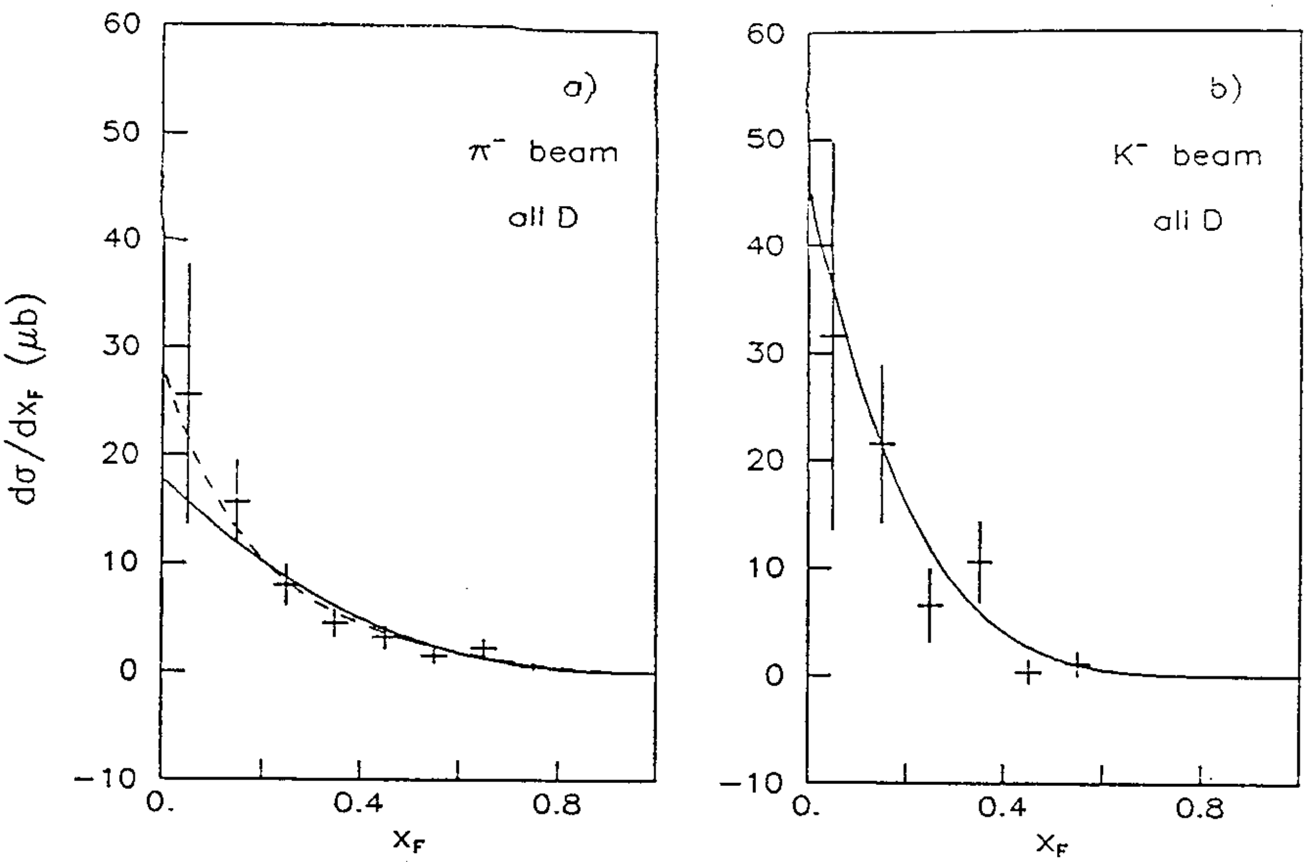

a)
π⁻ beam
all D
b)
K⁻ beam
all D
dσ/dx_F (μb)
x_F
60
50
40
30
20
10
0
−10
0.
0.4
0.8

Fig.5

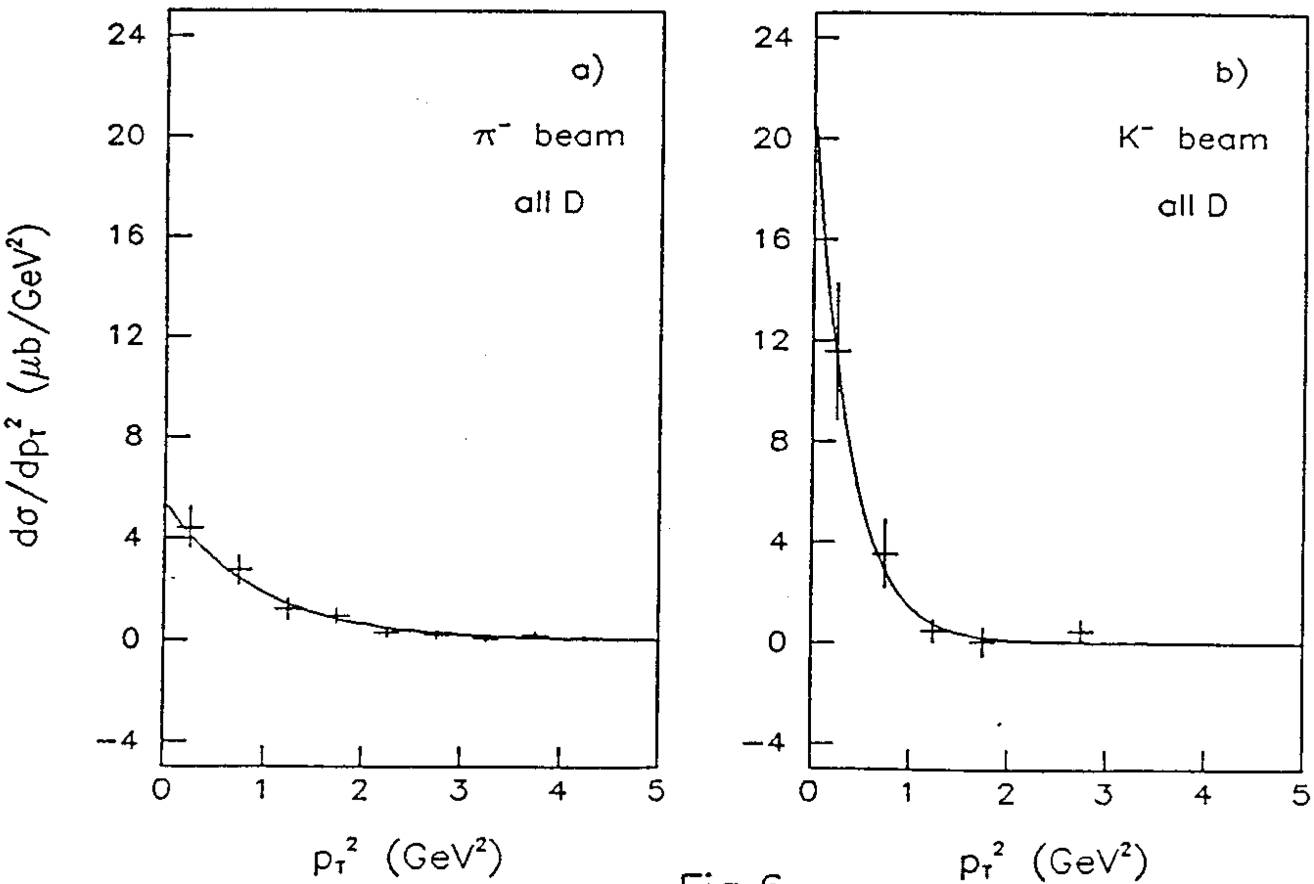

a)
π⁻ beam
all D
b)
K⁻ beam
all D
dσ/dp_T² (μb/GeV²)
p_T² (GeV²)
24
20
16
12
8
4
0
−4
0
1
2
3
4
5

Fig.6

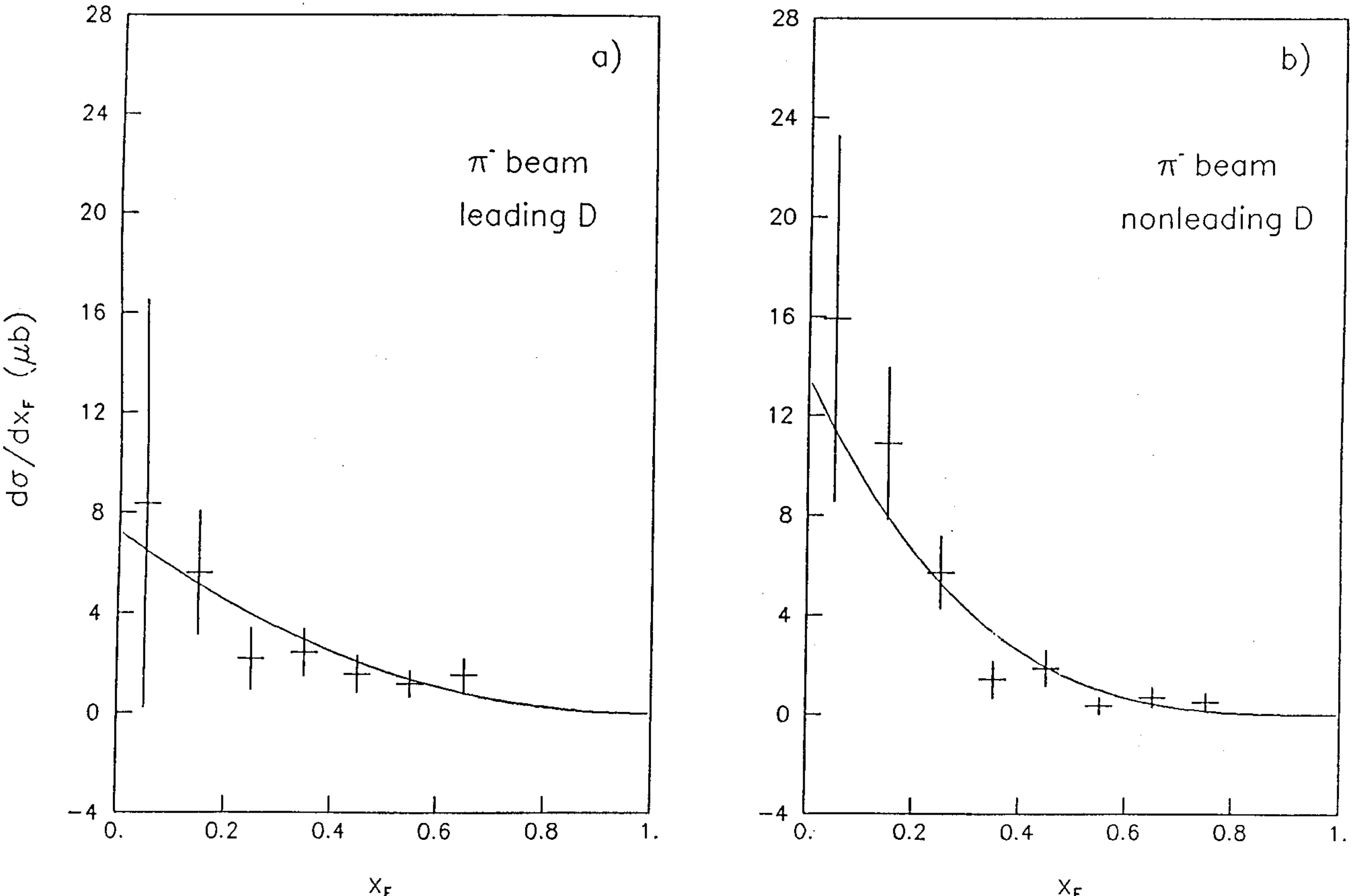
a)
π⁻ beam
leading D
b)
π⁻ beam
nonleading D
dσ/dx_F (μb)
x_F
28
24
20
16
12
8
4
0
−4
0.
0.2
0.4
0.6
0.8
1.

Fig.7

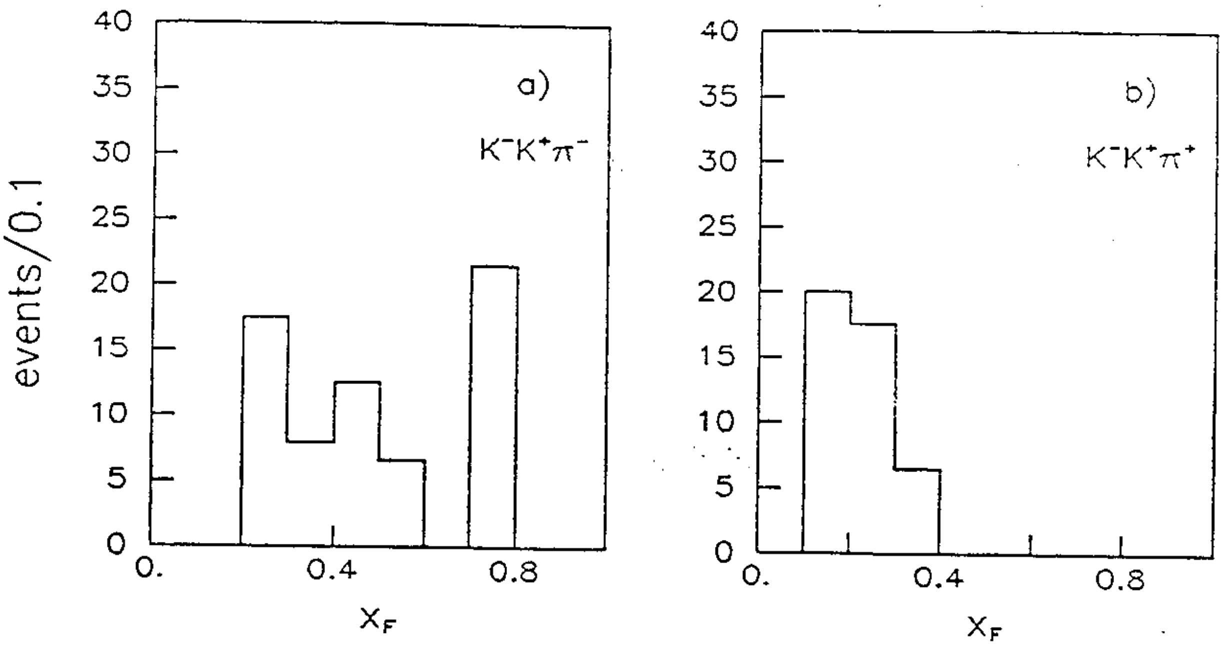

Fig.8

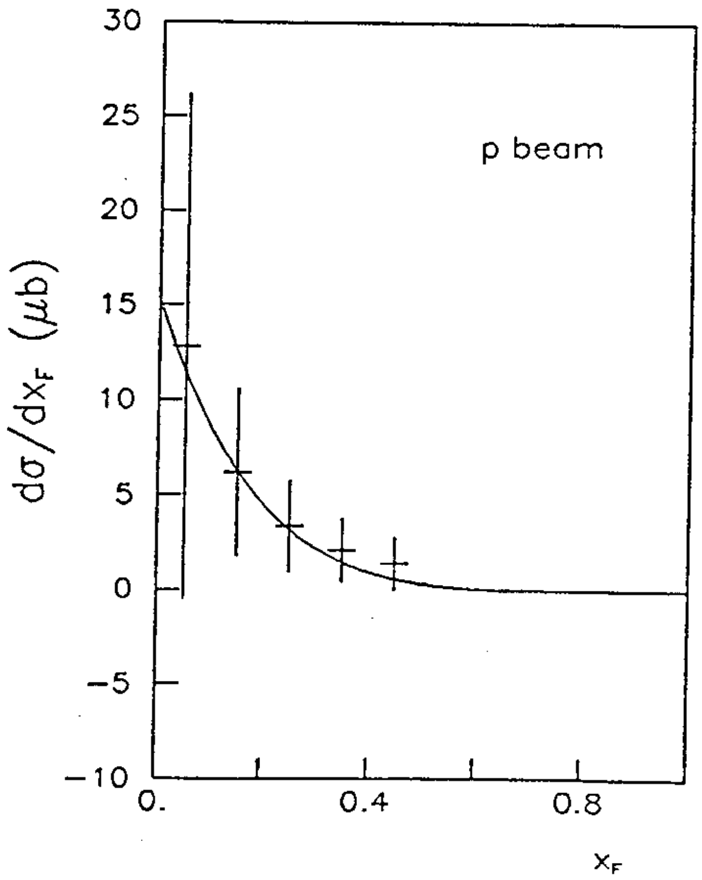

Fig.9

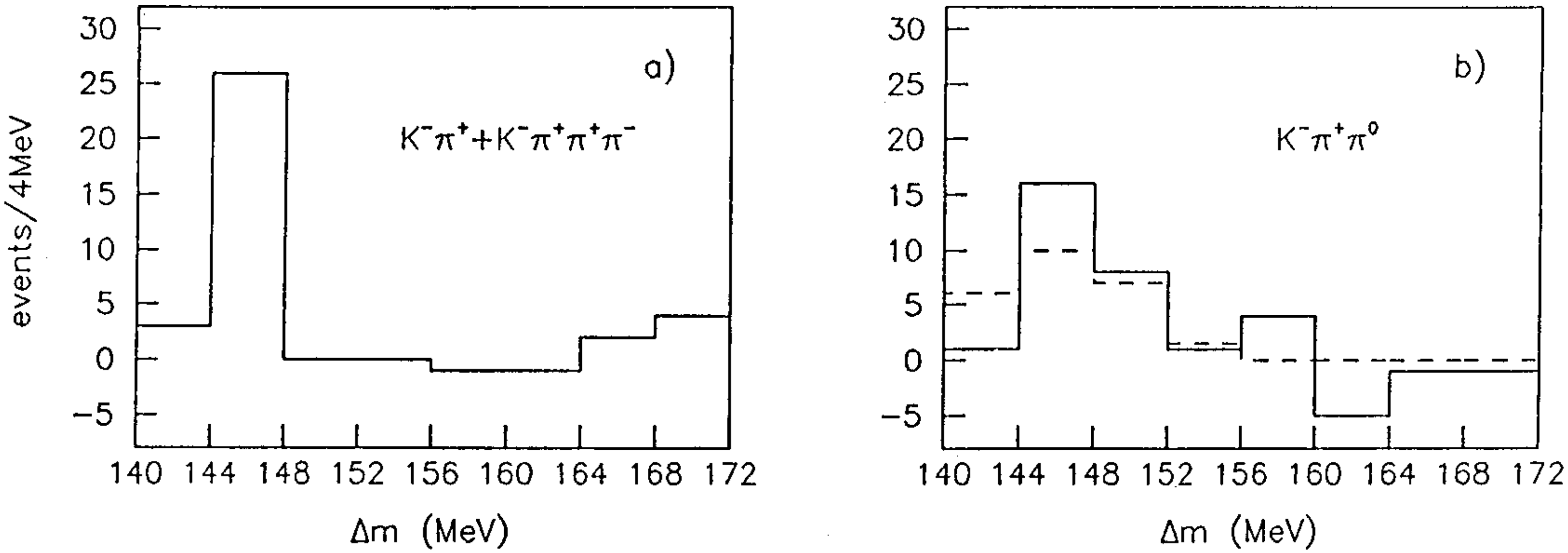
events/4MeV
a)
K⁻π⁺+K⁻π⁺π⁺π⁻
b)
K⁻π⁺π⁰
Δm (MeV)
Δm (MeV)

Fig.10

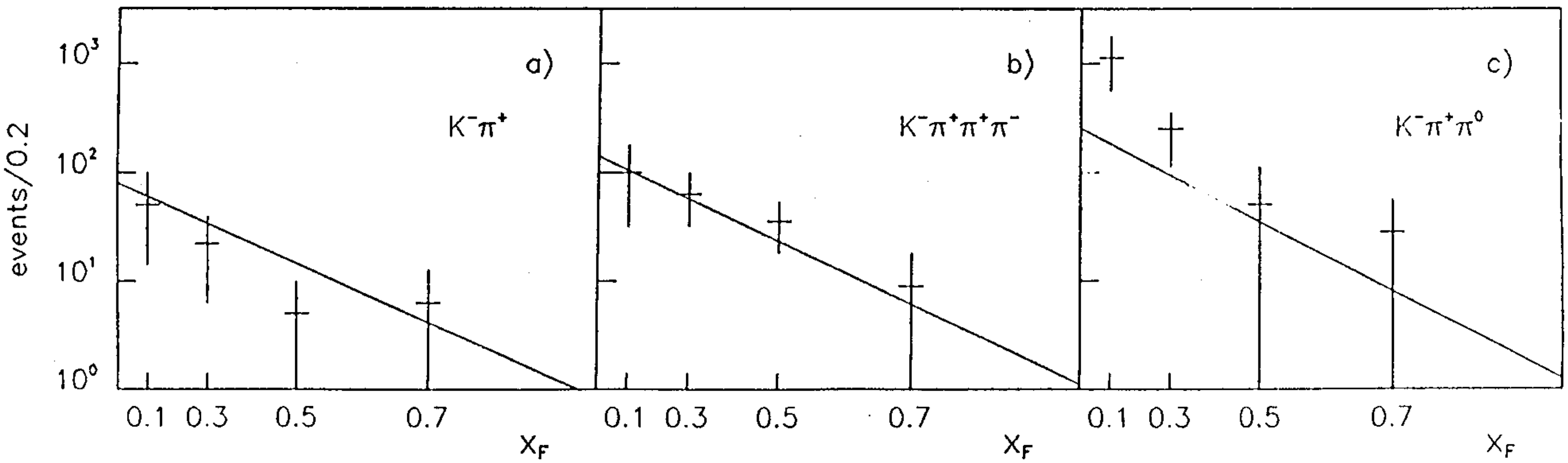
events/0.2
a)
K⁻π⁺
b)
K⁻π⁺π⁺π⁻
c)
K⁻π⁺π⁰
X_F
X_F
X_F

Fig.11

Druck: Dokumentationsstelle des Max-Planck-Instituts für Physik und Astrophysik, 8046 Garching